
Structured Pruning is All You Need for Pruning CNNs at Initialization

Yaohui Cai Weizhe Hua Hongzheng Chen
G. Edward Suh Christopher De Sa Zhiru Zhang
Cornell University

{yc2632, wh399, hc676, gs272, cmd353, zhiruz}@cornell.edu

Abstract

Pruning-at-initialization (PAI) proposes to prune the individual weights of the CNN before training, thus avoiding expensive fine-tuning or retraining of the pruned model. While PAI shows promising results in reducing model size, the pruned model still requires unstructured sparse matrix computation, making it difficult to achieve wall-clock speedups. In this work, we show theoretically and empirically that the accuracy of CNN models pruned by PAI methods only depends on the fraction of remaining parameters in each layer (i.e., *layer-wise density*), regardless of the granularity of pruning. We formulate the PAI problem as a convex optimization of our newly proposed expectation-based proxy for model accuracy, which leads to finding the optimal layer-wise density of that specific model. Based on our formulation, we further propose a structured and hardware-friendly PAI method, named PreCrop, to prune or reconfigure CNNs in the channel dimension. Our empirical results show that PreCrop achieves a higher accuracy than existing PAI methods on several modern CNN architectures, including ResNet, MobileNetV2, and EfficientNet for both CIFAR-10 and ImageNet. PreCrop achieves an accuracy improvement of up to 2.7% over the state-of-the-art PAI algorithm when pruning MobileNetV2 on ImageNet. PreCrop also improves the accuracy of EfficientNetB0 by 0.3% on ImageNet with only 80% of the parameters and the same FLOPs.

1 Introduction

Convolutional neural networks (CNNs) have achieved state-of-the-art accuracy in a wide range of machine learning (ML) applications. However, the massive computational and memory requirements of CNNs remain a major barrier to more widespread deployment on resource-limited edge and mobile devices. This challenge has motivated a large body of research on CNN compression in order to simplify the original model without significantly compromising accuracy.

Weight pruning [15, 7, 18, 4, 8] is one of the most extensively explored methods to reduce the computational and memory demands of CNNs. Existing weight pruning approaches create a sparse CNN model by iteratively removing ineffective weights or activations and training the resulting sparse model. Moreover, training-based pruning methods introduce additional hyperparameters, such as the learning rate for fine-tuning and the number of epochs before rewinding [21], leading to a more complicated and less reproducible pruning process. Among the different pruning techniques, training-based pruning usually enjoys the least accuracy degradation but at the cost of an expensive pruning procedure.

To minimize the cost of pruning, a new line of research proposes *pruning-at-initialization (PAI)* [16, 28, 25], which identifies and prunes unimportant weights in a CNN right after initialization but before training. As in training-based pruning methods, PAI evaluates the importance score of each individual weight and retains only a subset of weights by maximizing the sum of the importance scores of all remaining weights. The compressed model is then trained using the same hyperparameters (e.g.,

Preprint. Under review.

weight decaying factor) for the same number of epochs as the baseline model. Thus, the pruning and training of CNNs are cleanly decoupled, which greatly reduces the complexity of obtaining a pruned CNN model. Currently, SynFlow [25] is considered the state-of-the-art PAI technique – it further eliminates the need for data in pruning as required in [16, 28] and achieves higher accuracy with the same number of parameters.

However, existing PAI methods mostly focus on fine-grained weight pruning, which removes individual weights from the CNN model without preserving any structure. As a result, inference and training of the pruned model require sparse matrix computation, which is challenging to accelerate on commercially-available ML hardware such as GPUs and TPUs [14] that are optimized for dense computation. According to a recent study [6], even with the NVIDIA cuSPARSE library, one can only achieve a meaningful speedup for sparse matrix multiplications on GPUs when the sparsity is over 98%. In practice, it is difficult for modern CNNs to shrink by more than $50\times$ without a drastic degradation in accuracy [2]. Structural pruning patterns (e.g., pruning weights for the entire output channel) are needed to avoid irregularly sparse storage and computation, thus providing practical memory and computational savings. Moreover, recent studies [23, 5] also observe that randomly shuffling the binary weight mask of each layer or reinitializing all remaining weights does not affect the accuracy of the model compressed using existing PAI methods. In this work, we first review the limitations of all previous PAI methods,

Based on the observations, we hypothesize that existing PAI methods are only effective in determining the fraction of remaining weights in each layer, but fail to find a significant subset of weights. We propose to use the expectation of the sum of importance scores of all weights, rather than the sum, as a proxy for the accuracy of the model, thus treating all weights in the same layer with equal importance. With our new proxy for accuracy named **SynExp** (Synaptic Expectation), we can formulate PAI as a convex optimization problem that directly solves the optimal fraction of remaining weights per layer (i.e., *layer density*) subject to certain model size and/or FLOPs constraints. We also prove a theorem that SynExp does not change the same as long as the layer-wise density remains the same, regardless of the granularity of pruning. The theorem opens an important opportunity that coarse-grained PAI methods can achieve similar accuracy as their existing fine-grained counterparts such as SynFlow. We demonstrate the efficacy of the proposed proxy through extensive empirical experiments.

We further propose **PreCrop**, a structured PAI that prunes CNN models at the channel level. PreCrop can effectively reduce the model size and computational cost without loss of accuracy compared to fine-grained PAI methods, and more importantly, provide a wall-clock speedup on commodity hardware. By allowing each layer to have more parameters than the baseline network, we are also able to *reconfigure* the width dimension of the network with almost zero cost, which is termed **PreConfig**. Our empirical results show that the model after PreConfig can achieve higher accuracy with fewer parameters and FLOPs than the baseline for a variety of modern CNNs.

We summarize our contributions as follows:

- We propose to use the expectation of the sum of importance scores of all weights as a proxy for accuracy and formulate PAI as a SynExp optimization problem constrained by the model size and/or FLOPs. We also prove that the accuracy of the CNN model pruned by solving the constrained optimization is independent of the pruning granularity.
- We introduce PreCrop to prune CNNs at the channel level based on the proposed SynExp optimization. Our empirical study demonstrates that models pruned using PreCrop achieve similar or better accuracy compared to the state-of-the-art unstructured PAI approaches while preserving regularity. Compared to SynFlow, PreCrop achieves 2.7% and 0.9% higher accuracy on MobileNetV2 and EfficientNet on ImageNet with fewer parameters and FLOPs.
- We show that PreConfig can be used to optimize the width of each layer in the network with almost zero cost (e.g., the search can be done within one second on a CPU). Compared to the original model, PreConfig achieves 0.3% accuracy improvement with 20% fewer parameters and the same FLOPs for EfficientNet and MobileNetV2 on ImageNet.

2 Related Work

Model Compression in General can reduce the computational cost of large networks to ease their deployment in resource-constrained devices. Besides pruning, quantization [3, 31, 13], NAS [32, 24], and distillation [12, 29] are also commonly used to improve the model efficiency.

Training-Based Pruning uses various heuristic criteria to prune unimportant weights. They typically require an iterative training-prune-retrain process where the pruning stage is intertwined with the training stage, which may increase the overall training cost by several folds. Because pruning aims to reduce parameters, the FLOPs reduction is usually less significant [17, 4].

Existing training-based pruning methods can be either unstructured [7, 15] or structured [11, 19], depending on the granularity and regularity of the pruning scheme. Training-based unstructured pruning usually provides a better accuracy-size trade-off while structured pruning can achieve a more practical speedup and compression without special support of custom hardware.

(Unstructured) Pruning-at-Initialization (PAI) [16, 28, 25] provides a promising approach to mitigating the high cost of training-based pruning.

They can identify and prune unimportant weights right after initialization and before the training starts. Related to these efforts, authors of [5] and [23] independently find that for all existing PAI methods, randomly shuffling the weight mask within a layer or reinitializing all the weights in the network does not cause any accuracy degradation.

Neural Architecture Search (NAS) [32, 27] automatically searches over a large set of candidate models to achieve the optimal accuracy-computation trade-off. The search space of NAS usually includes width, depth, resolution, and choice of building blocks. However, existing approaches can only search in a small subset of the possible channel width configurations due to the cost. The cost for NAS is also orders of magnitude higher than training a model. Some NAS algorithms [1, 30] use a cheap proxy instead of training the whole network, but an expansive reinforcement learning [32] or evolutionary algorithm [20] is still used to predict a good network.

3 Pruning-at-initialization via SynExp Optimization

In this section, we first discuss the preliminaries and limitations of existing PAI methods. We propose a new proxy for the accuracy of the compressed model to overcome these limitations. With the proposed proxy, we formulate the PAI problem into a convex optimization problem.

3.1 Preliminaries and Limitations of PAI

Preliminaries. PAI aims to prune neural networks after initialization but before training to avoid the time-consuming *training-pruning-retraining* process. Prior to training, PAI uses the gradients with respect to the weights to estimate the importance of individual weights, which requires forward and backward propagations. Weights (W) with smaller importance scores are pruned by setting the corresponding entries in the binary weight mask (M) to zero. Existing PAI methods, such as SNIP [16], GraSP [28], and SynFlow [25] mainly explore different methods to estimate the importance of individual weights. Single-shot PAI algorithms, such as SNIP and GraSP, prune the model to the desired sparsity in a single pass. Alternatively, SynFlow, which represents the state-of-the-art PAI algorithm, repeats the process of pruning a small fraction of weights and re-evaluating the importance scores until the desired pruning rate is reached. Through the iterative process, the importance of weights can be estimated more accurately.

Specifically, the importance score used in SynFlow can be formulated as:

$$\mathcal{S}_{\text{SF}}(W_{ij}^l) = \left[\mathbf{1}^T \prod_{k=l+1}^N |W^k \odot M^k| \right]_i |W_{ij}^l M_{ij}^l| \left[\prod_{k=1}^{l-1} |W^k \odot M^k| \mathbf{1} \right]_j, \quad (1)$$

where N is the number of layers, W^l and M^l are the weight and weight mask of the l -th layer, $\mathcal{S}_{\text{SF}}(W_{ij}^l)$ is the SynFlow score for a single weight W_{ij}^l , \odot denotes the Hadamard product, $|\cdot|$ is element-wise absolute operation, and $\mathbf{1}$ is an all-one vector. It is worth noting that none of the data or labels is used to compute the importance score, thus making SynFlow a data-agnostic algorithm.

Limitations. As pointed out by [23, 5], randomly shuffling the weight mask W of each layer or reinitializing all the weights M does not affect the final accuracy of models compressed using existing PAI methods. In addition, they show that given the same layer-wise density (i.e., the fraction of remaining weights in each layer), the pruned models will have similar accuracy. The observations suggest that even though the existing PAI algorithms try to identify less important weights, which weights to prune is not important for accuracy.

All previous PAI methods use the *sum* of importance scores of the remaining weights as a proxy for model accuracy, which is identical to the training-based pruning [7, 15]. PAI obtains the binary weight mask by maximizing the proxy as follows

$$\text{maximize } \sum_{l=1}^N S^l \cdot M^l \quad \text{over } M \quad \text{subject to } \sum_{l=1}^N \|M^l\|_0 \leq B_{\text{params}}, \quad (2)$$

where N is the number of layers in the network, S^l is the score matrix in the l -th layer, M^l is the binary weight mask in the l -th layer, $\|\cdot\|_0$ is the number of nonzero entries in a matrix, and B_{params} is a pre-defined model size constraint.

Regardless of the specific PAI importance score chosen, a subset of weights is determined to be more important than the other weights, which contradicts the observation that random shuffling does not affect accuracy. Instead, we propose a new accuracy proxy for PAI to address the limitations.

3.2 SynExp Invariance Theorem

Inspired by the observations of previous PAI methods, we conjecture that a proxy for the accuracy of the model pruned using a PAI method should satisfy the following two properties:

1. The pruning decision (i.e., weight mask M) can be made *before* the model is initialized.
2. Maximization of the proxy should result in optimal *layer-wise density*, not pruning decisions for individual weights.

For random pruning before initialization, given a fixed density p_l for each layer, the weight matrix W_l and the binary mask matrix M_l of that layer can be considered two random variables. The binary weight mask is applied to the weight matrix element-wisely as $W_l \odot M_l$, where \odot represents Hadamard product. The weight matrix of layer l (i.e., W^l) contains α_l parameters. Each individual weight in layer l is sampled independently from a given distribution D^l . Suppose $A^l = \{M, M_i \in \{0, 1\} \forall 1 \leq i \leq \alpha_l, \sum_i M_i = p_l \times \alpha_l\}$ is the set of all possible binary matrices with the same shape as the weight matrix W^l that satisfy the layer-wise density (p_l) constraint. Then, the random weight mask M^l for layer l is sampled uniformly from A^l .

Let $M = \{M^l, \forall 1 \leq l \leq N\}$ and $W = \{W^l, \forall 1 \leq l \leq N\}$ be the weights and masks of all N layers in the network, respectively. The observations in Section 3.1 indicate that any instantiation of the two random variables M and W results in similar final accuracy of the pruned model. However, the different instantiations do change the proxy value for the model accuracy in existing PAI methods. For example, the SynFlow score in Equation 2 changes under different instances of M and W . Therefore, we propose a new proxy that is invariant to the instantiations of M and W for the model accuracy in the context of PAI — the *expectation* of the sum of the importance scores of all unpruned (i.e., remaining) weights. The proposed proxy can be formulated as follows:

$$\text{maximize } \mathbb{E}_{M,W}[\mathcal{S}] = \mathbb{E}_{M,W} \left[\sum_{l=1}^N S^l \cdot M^l \right] \quad \text{over } p_l \quad \text{subject to } \sum_{l=1}^N \alpha_l \cdot p_l \leq B_{\text{params}}, \quad (3)$$

where p_l represents layer-wise density of layer l , α_l is the number of parameters in layer l , $\mathbb{E}_{M,W}[\mathcal{S}]$ stands for the expectation of the importance score \mathcal{S} over random weight W , and binary random mask M . In this new formulation, the layer-wise density p_l is optimized to maximize the proposed proxy for model accuracy.

In order to evaluate the expectation before weight initialization, we adopt the importance metric proposed by SynFlow, i.e., replacing \mathcal{S} in Equation 3 with \mathcal{S}_{SF} in Equation 1. As a result, we can compute the expectation analytically without forward or backward propagations. This new expectation-based proxy is referred to as *SynExp* (Synaptic Expectation). We further prove SynExp

is invariant to the granularity of PAI in the SynExp Invariance Theorem. The detailed proof can be found in Appendix A.

Theorem 1. *Given a specific CNN architecture, the SynExp ($\mathbb{E}_{[M,W]}[\mathcal{S}_{SF}]$) of any randomly compressed model with the same layer-wise density p_l is a constant, independent of the pruning granularity. The constant SynExp equals to:*

$$\mathbb{E}_{M,W}[\mathcal{S}_{SF}] = NC_{N+1} \prod_{l=1}^N (p_l C_l \cdot \mathbb{E}_{x \sim \mathcal{D}}[|x|]), \quad (4)$$

where N is the number of layers in the network, $\mathbb{E}_{x \sim \mathcal{D}}[|x|]$ is the expectation of magnitude of distribution \mathcal{D} , C_l is the input channel size of layer l and is also the output channel size of $l - 1$, and $p_l = \frac{1}{\alpha_l} \|M_l\|_0$ is the layer-wise density.

In Equation 4, N and C^l are all hyperparameters of the CNN architecture and can be considered constants. $\mathbb{E}_{\mathcal{D}^l}$ is also a constant under a particular distribution \mathcal{D}^l . The layer-wise density p_l is the only variable that needs to be solved in the equation. Thus, SynExp satisfies both of the aforementioned properties: 1) pruning is done prior to the weight initialization; 2) the layer-wise density can be directly optimized. Furthermore, Theorem 1 also shows that the granularity of pruning has no impact on the proposed SynExp metric. In other words, the CNN models compressed using unstructured and structured pruning methods will have similar accuracy.

We empirically verify Theorem 1 by randomly pruning each layer of a CNN with different pruning granularity but the same layer-wise density (p_l). In this empirical study, we perform random pruning with three different granularities (i.e., weight, filter, and channel) to achieve the desired layer-wise density obtained from solving Equation 3. For weight and filter pruning, randomly pruning each layer to match the layer-wise density p_l occasionally detaches some weights from the network, especially when the density is low. The detached weights do not contribute to the prediction but are counted as remaining parameters. Thus, we remove the detached weights for a fair comparison following [26]. For channel pruning, it is non-trivial to achieve the given layer-wise density while satisfying the constraint that the output channel size of the previous layer should be equal to the input channel size of the next layer. Therefore, we use PreCrop proposed in Section 4.2. As shown in Figure 1, random pruning with different granularity can obtain similar accuracy compared to SynFlow, as long as the layer-wise density remains the same. The empirical results are consistent with Theorem 1 and also demonstrate the efficacy of the proposed SynExp metric. We include more empirical results for different CNN architectures and different importance scores in Appendix C.

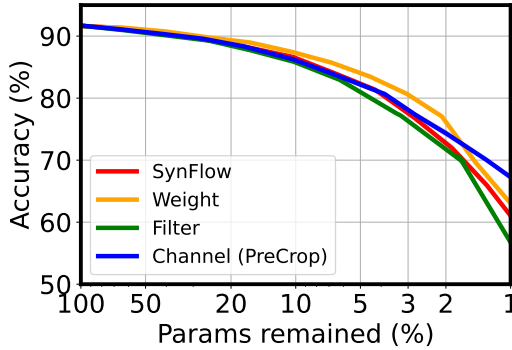


Figure 1: Comparison of the performance using different pruning granularities on ResNet20 using CIFAR-10.

3.3 Optimizing SynExp

As discussed in Section 3.2, only the layer-wise density matters for our proposed SynExp approach. Here, we show how to obtain the layer-wise density in Equation 3 that maximizes SynExp under model size and/or FLOPs constraints.

3.3.1 Optimizing SynExp with Parameter Count Constraint

Given that the goal of PAI is to reduce the size of the model, we need to add an additional constraint on the total number of parameters B_{params} (i.e., parameter constraint), where B_{params} is typically greater than zero and less than the number of parameters in the original network. Since layer-wise density p_l is the only variable in Equation 3, we can simplify the equation by removing all other

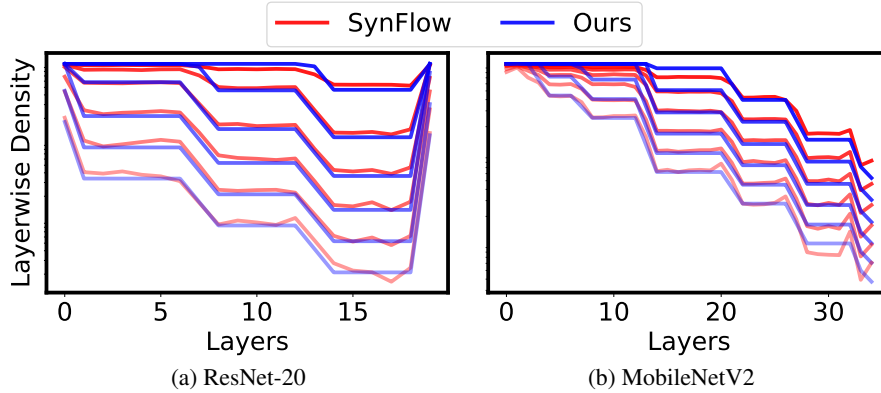


Figure 2: Comparison of the layer-wise densities obtained by SynExp optimization with parameter count constraint and SynFlow. Higher transparency means that the problem is constrained by a smaller parameter count.

constant terms, as follows:

$$\begin{aligned} \text{maximize } \sum_{l=1}^N \log p_l \quad \text{over } p_l \quad \text{subject to } \sum_{l=1}^N \alpha_l \cdot p_l \leq B_{\text{params}}, \\ 0 < p_l \leq 1, \forall 1 \leq l \leq N, \end{aligned} \quad (5)$$

where α_l is the number of parameters in layer l .

Equation 5 is a convex optimization problem that can be solved analytically¹. We compare the layer-wise density derived from solving Equation 5 with the density obtained using SynFlow. As shown in Figure 2, the layer-wise density obtained by both approaches are nearly identical, where our new formulation gets rid of the iterative re-evaluation of SynFlow scores and the pruning process in SynFlow. It is also worth noting that the proposed method finds the optimal layer-wise density even before the network is initialized.

3.3.2 Optimizing SynExp with Parameter Count and FLOPs Constraints

As discussed in Section 3.3.1, we can formulate PAI as a simple convex optimization problem with a constraint on the model size. However, the number of parameters does not always reflect the performance (e.g., throughput) of the CNN model. In many cases, CNN models are compute-bound on many commodity hardwares [14, 9]. Therefore, we propose to also introduce a FLOPs constraint in our formulation.

The FLOPs saved in existing PAI algorithms specified in Equation 2 come from pruning the weights in the CNN model. In other words, given a parameter constraint, the FLOP count of the pruned model is also determined. It is not straightforward to introduce a FLOP constraint for each layer in the model, because the correspondence between the number of parameters and FLOPs varies across different layers. Therefore, none of the existing PAI methods can be directly used to bound the FLOPs of CNN models. Since the weights in the same layer are associated with the same FLOP count, we can directly incorporate the constraint on FLOPs B_{FLOPs} (i.e., FLOPs constraint) into the convex optimization problem as follows:

$$\begin{aligned} \text{maximize } \sum_{l=1}^N \log p_l \quad \text{over } p_l \quad \text{subject to } \sum_{l=1}^N \alpha_l \cdot p_l \leq B_{\text{params}}, \sum_{l=1}^N \beta_l \cdot p_l \leq B_{\text{FLOPs}} \\ 0 < p_l \leq 1, \forall 1 \leq l \leq N, \end{aligned} \quad (6)$$

where β_l is the number of FLOPs in the l^{th} layer.

Since the additional FLOPs constraint is linear, the optimization problem in Equation 6 remains convex and has an analytical solution¹. By solving SynExp optimization with a fixed B_{params} but different B_{FLOPs} , we can obtain the layer-wise density for various models that have the same number of parameters but different FLOPs. Then, we perform random weight pruning on the CNN model to

¹We include analytical solutions for Equation 5 and Equation 6 in Appendix B for completeness.

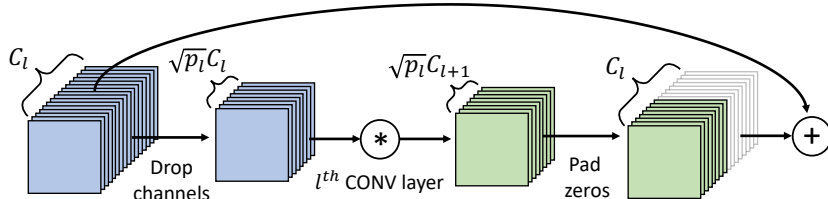


Figure 4: Illustration of PreCrop for layers with residual connections — C_l and C_{l+1} represent the number of input channels of layer l and $l + 1$, respectively. p_l represents the density of layer l .

achieve the desired layer-wise density. We compare the proposed SynExp optimization (denoted as Ours) with other popular PAI methods. As depicted in Figure 3, given a fixed model size (1.5×10^4 in the figure), our method can be used to generate a Pareto Frontier that spans the spectrum of FLOPs, while other methods can only have a fixed FLOPs. Our method dominates all other methods in terms of both accuracy and FLOPs reduction.

4 Structured Pruning-at-Initialization

The SynExp Invariance Theorem shows that pruning granularity of PAI methods should not affect the accuracy of the pruned model. Channel pruning, which prunes the weights of the CNN at the output channel granularity, is considered the most coarse-grained and hardware-friendly pruning technique. Therefore, applying the proposed PAI method for channel pruning can avoid both complicated retraining/re-tuning procedures and irregular computations. In this section, we propose a structured PAI method for channel pruning, named PreCrop, to prune CNNs in the channel dimension. In addition, we propose a variety of PreCrop with relaxed density constraints to reconfigure the width of each layer in the CNN model, which is called PreConfig.

4.1 PreCrop

Applying the proposed PAI method to channel pruning requires a two-step procedure. First, the layer-wise density p_l is obtained by solving the optimization problem shown in Equation 5 or 6. Second, we need to decide how many output channels of each layer should be pruned to satisfy the layer-wise density. However, it is not straightforward to compress each layer to match a given layer-wise density due to the additional constraint that the number of output channels of the current layer must match the number of input channels of the next layer.

We introduce PreCrop, which compresses each layer to meet the desired layer-wise density. Let C_l and C_{l+1} be the number of input channels of layer l and $l + 1$, respectively. C_{l+1} also means the number of output channels of layer l . For layers with no residual connections, the number of output channels of layer l is reduced to $\lfloor \sqrt{p_l} \cdot C_{l+1} \rfloor$. The number of input channels of layer $l + 1$ needs to match the number of output channels of layer l , which is also reduced to $\lfloor \sqrt{p_l} \cdot C_{l+1} \rfloor$. Therefore, the actual density of layer l after PreCrop is $\sqrt{p_{l-1} \cdot p_l}$ instead of p_l . We empirically find that $\sqrt{p_{l-1} \cdot p_l}$ is close enough to p_l because the neighboring layers have similar layer-wise densities. Alternatively, it is possible to obtain the exact layer-wise density p by only reducing the number of input or output channels of a layer. However, this approach leads to a significant drop in accuracy, because the number of the input and output channels can change dramatically (e.g., $p_l C_l \ll C_{l+1}$ or $C_l \gg p_l C_{l+1}$). This causes the shape of the feature map changes dramatically in adjacent layers, resulting in information loss.

For layers with residual connections, Figure 4 depicts an approach to circumvent the constraint on the number of channels of adjacent layers. We can reduce the number of input and output channels of layer l from C_l and C_{l+1} to $\sqrt{p_l}C_l$ and $\sqrt{p_l}C_{l+1}$, respectively. In this way, the density of each layer can match the given layer-wise density obtained from the proposed PAI method. Since the output of layer l needs to be added element-wisely with the original input to layer l , the output of layer l is

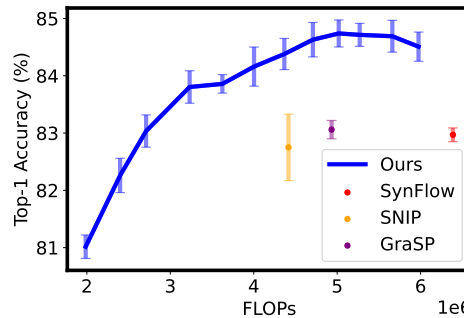


Figure 3: Comparison of our method with other PAI methods — we repeat the experiment using ResNet-20 on CIFAR-10 five times and report the mean and variance (error bar) of the accuracy. All the models in the figures have 1.5×10^4 parameters.

padding with zero-valued channels to match the shape of the original input. In our implementation, we simply add the output of layer l to the first $\sqrt{p_l}C_{l+1}$ channels of the original input to layer l , thus requiring no extra memory or computation for zero padding. PreCrop eliminates the requirement for sparse computation in existing PAI methods and thus can be used to accelerate both training and inference of the pruned models.

4.2 PreConfig: PreCrop with Relaxed Density Constraint

PreCrop uses the layer-wise density obtained from solving the convex optimization problem, which is always less than 1 following the common setting for pruning (i.e., $p_l < 1$). However, this constraint on layer-wise density is not necessary for our method since we can increase the number of channels (i.e., expand the width of the layer) before initialization. By solving the problem in Equation 6 without the constraint $p_l \leq 1$, we can expand the layers with a density greater than 1 ($p_l > 1$) and prune the layers with a density less than 1 ($p_l < 1$). We call this variant of PreCrop as PreConfig (PreCrop-Reconfigure). If we set B_{params} and B_{FLOPs} to be the same as the original network, we can essentially reconfigure the width of each layer of a given network architecture under certain constraints on model size and FLOPs.

The width of each layer in a CNN is usually designed manually, which often relies on extensive experience and intuition. Using PreConfig, we can determine the width of each layer in the network to achieve a better cost-accuracy tradeoff. PreConfig can also be used as an or a part of an ultra-fast NAS. Compared to NAS, which typically searches on the width, depth, resolution, and choice of building blocks, PreConfig only changes the width. Nonetheless, PreConfig only requires a minimum amount of time and computation compared to NAS methods; it only needs to solve a relatively small convex optimization problem, which can be solved in a second on a CPU.

5 Evaluation

In this section, we empirically evaluate PreCrop and PreConfig. We first demonstrate the effectiveness of PreCrop by comparing it with SynFlow. We then use PreConfig to tune the width of each layer and compare the accuracy of the model after PreConfig with the original model. We perform experiments using various modern CNN models, including ResNet [10], MobileNetV2 [22], and EfficientNet [24], on both CIFAR-10 and ImageNet. We set all hyperparameters used to train the models pruned by different PAI algorithms to be the same. See Appendix E for detailed hyperparameter settings.

5.1 Evaluation of PreCrop

For CIFAR-10, we compare the accuracy of SynFlow (red line) and two variants of PreCrop: PreCrop-Params (blue line) and PreCrop-FLOPs (green line). PreCrop-Params adds the parameter count constraint whereas PreCrop-FLOPs imposes the FLOPs constraint into the convex optimization problem. As shown in Figure 5a, PreCrop-Params achieves similar or even better accuracy as SynFlow under a wide range of different model size constraints, thus validating that PreCrop-Params can be as effective as the fine-grained PAI method. Considering the benefits of structured pruning, PreCrop-Params should be favored over existing PAI methods. Figure 5b further shows that PreCrop-FLOPs consistently outperforms SynFlow by a large margin, especially when the reduction in FLOPs is large. The experimental results show that PreCrop-FLOPs should be adopted when the performance of the model is limited by the computational cost.

Table 1 summarizes the comparison between PreCrop and SynFlow on ImageNet. For ResNet-34, PreCrop achieves 0.6% lower accuracy compared to SynFlow with a similar model size and FLOPs. For both MobileNetV2 and EfficientNetB0, PreCrop achieves 1.2% and 0.9% accuracy improvements compared to SynFlow with strictly fewer FLOPs and parameters, respectively. The experimental results on ImageNet further support SynExp Invariance Theorem that a coarse-grained structured pruning (e.g., PreCrop) can perform as well as unstructured pruning. In conclusion, PreCrop achieves a favorable accuracy and model size/FLOPs tradeoff compared to the state-of-the-art PAI algorithm.

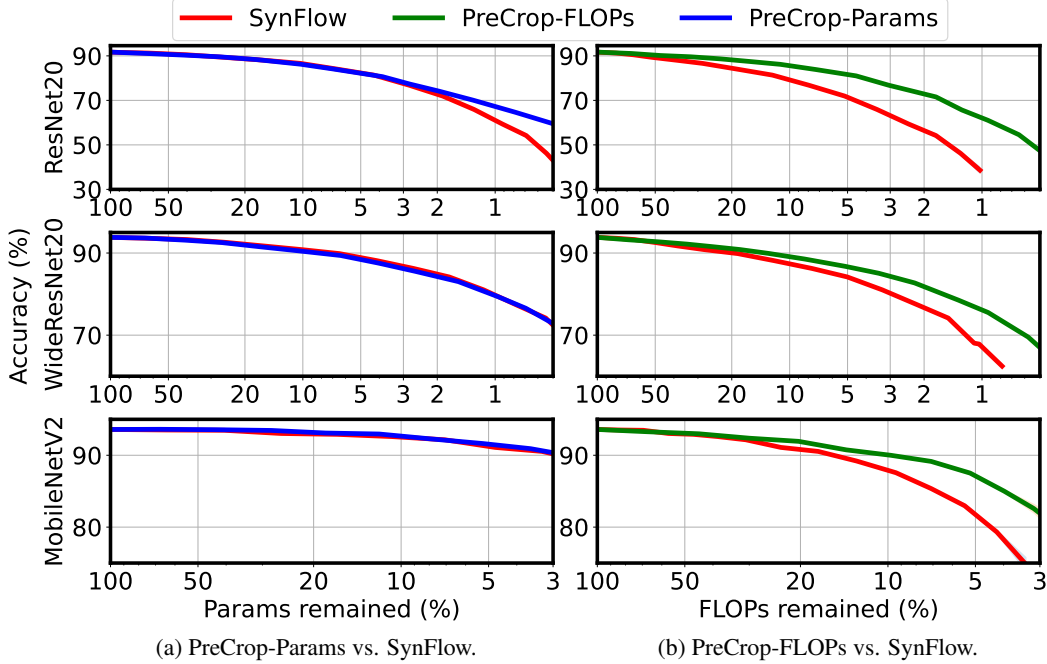


Figure 5: Comparison of PreCrop-Params and PreCrop-FLOPs with SynFlow — we repeat the experiment using ResNet20 (top), WideResNet20 (middle), and MobileNetV2 (bottom) on CIFAR-10 three times and report the mean and variance (error bar) of the accuracy.

Table 1: **Comparison of PreCrop with SynFlow on ImageNet** — The dagger([†]) implies that the numbers are only theoretical without considering the overhead of storing sparse matrices.

NETWORK	METHODS	FLOPs (G)	PARAMS (M)	ACCURACY (%)
RESNET34	BASELINE	3.64	21.80	73.5
	SYNFLOW	2.78 [†] (76.4%)	10.91[†] (50.0%)	72.1 (-1.4)
	PRECROP	2.73 (75.0%)	11.09 (50.8%)	71.5 (-2.0)
MOBILENETV2	BASELINE	0.33	3.51	69.6
	SYNFLOW	0.26[†] (78.8%)	2.44 [†] (68.6%)	67.6 (-2.0)
	PRECROP	0.26 (78.8%)	2.33 (66.4%)	68.8 (-0.8)
	SYNFLOW	0.21[†] (63.6%)	1.91 [†] (54.4%)	64.5 (-5.1)
	PRECROP	0.21 (63.6%)	1.85 (52.7%)	67.2 (-2.4)
EFFICIENTNETB0	BASELINE	0.40	5.29	73.0
	SYNFLOW	0.30[†] (75.0%)	3.72 [†] (70.3%)	71.8 (-1.2)
	PRECROP	0.30 (75.0%)	3.67 (69.4%)	72.7 (-0.3)

5.2 Evaluation of PreConfig

As discussed in Section 4.2, PreConfig can be viewed as an ultra-fast NAS technique, which adjusts the width of each layer in the model even before the weights are initialized.

Table 2 compares the accuracy of the reconfigured model with the original model under similar model size and FLOPs constraints. For ResNet34, with similar accuracy, we reduce the parameter count by 25%. For MobileNetV2, we achieve 0.3% higher accuracy than the baseline with 20% fewer parameters and 3% fewer FLOPs. For the EfficientNet, we can also achieve 0.3% higher accuracy than the baseline with only 80% of the parameters and the same FLOPs. Note that EfficientNet is identified by a NAS method. As PreConfig only changes the number of channels of the model before initialization, we believe it also applies to other compression techniques.

Table 2: PreConfig on ImageNet.

NETWORK	METHODS	FLOPs (G)	PARAMS (M)	ACCURACY (%)
RESNET	BASELINE	3.64	21.80	73.5
	PRECONFIG	3.64	16.52(75.8%)	73.3(-0.2)
MOBILENETV2	BASELINE	0.33	3.51	69.6
	PRECONFIG	0.32 (97.0%)	2.83(80.6%)	69.9(+0.3)
EFFICIENTNETB0	BASELINE	0.40	5.29	73.0
	PRECONFIG	0.40	4.29(81.1%)	73.3(+0.3)

6 Conclusion

In this work, we show theoretically and empirically that only the layer-wise density matters for the accuracy of the CNN models pruned using PAI methods. We formulate PAI as a simple convex SynExp optimization. Based on SynExp optimization, we further propose PreCrop and PreConfig to prune and reconfigure CNNs in the channel dimension. Our experimental results demonstrate that PreCrop can outperform existing fine-grained PAI methods on various networks and datasets.

References

- [1] Mohamed S Abdelfattah, Abhinav Mehrotra, Łukasz Dudziak, and Nicholas D Lane. Zero-cost proxies for lightweight nas. *arXiv preprint arXiv:2101.08134*, 2021.
- [2] Davis Blalock, Jose Javier Gonzalez Ortiz, Jonathan Frankle, and John Guttag. What is the state of neural network pruning? *arXiv preprint arXiv:2003.03033*, 2020.
- [3] Zhen Dong, Zhewei Yao, Yaohui Cai, Daiyaan Arfeen, Amir Gholami, Michael W Mahoney, and Kurt Keutzer. Hawq-v2: Hessian aware trace-weighted quantization of neural networks. *arXiv preprint arXiv:1911.03852*, 2019.
- [4] Jonathan Frankle and Michael Carbin. The lottery ticket hypothesis: Finding sparse, trainable neural networks. *arXiv preprint arXiv:1803.03635*, 2018.
- [5] Jonathan Frankle, Gintare Karolina Dziugaite, Daniel M Roy, and Michael Carbin. Pruning neural networks at initialization: Why are we missing the mark? *arXiv preprint arXiv:2009.08576*, 2020.
- [6] Trevor Gale, Matei Zaharia, Cliff Young, and Erich Elsen. Sparse gpu kernels for deep learning. In *Proceedings of the International Conference for High Performance Computing, Networking, Storage and Analysis, SC '20*. IEEE Press, 2020.
- [7] Song Han, Huizi Mao, and William J Dally. Deep compression: Compressing deep neural networks with pruning, trained quantization and huffman coding. *arXiv preprint arXiv:1510.00149*, 2015.
- [8] Song Han, Jeff Pool, John Tran, and William Dally. Learning both weights and connections for efficient neural network. *Advances in neural information processing systems*, 28, 2015.
- [9] Pawan Harish and Petter J Narayanan. Accelerating large graph algorithms on the gpu using cuda. In *International conference on high-performance computing*, pages 197–208. Springer, 2007.
- [10] Kaiming He, Xiangyu Zhang, Shaoqing Ren, and Jian Sun. Deep residual learning for image recognition. In *Proceedings of the IEEE conference on computer vision and pattern recognition*, pages 770–778, 2016.
- [11] Yihui He, Xiangyu Zhang, and Jian Sun. Channel pruning for accelerating very deep neural networks. In *Proceedings of the IEEE international conference on computer vision*, pages 1389–1397, 2017.
- [12] Geoffrey Hinton, Oriol Vinyals, and Jeff Dean. Distilling the knowledge in a neural network. *arXiv preprint arXiv:1503.02531*, 2015.
- [13] Benoit Jacob, Skirmantas Kligys, Bo Chen, Menglong Zhu, Matthew Tang, Andrew Howard, Hartwig Adam, and Dmitry Kalenichenko. Quantization and training of neural networks for efficient integer-arithmetic-only inference. In *Proceedings of the IEEE conference on computer vision and pattern recognition*, pages 2704–2713, 2018.
- [14] Norman P. Jouppi, Cliff Young, Nishant Patil, David Patterson, Gaurav Agrawal, Raminder Bajwa, Sarah Bates, Suresh Bhatia, Nan Boden, Al Borchers, Rick Boyle, Pierre-luc Cantin, Clifford Chao, Chris Clark, Jeremy Coriell, Mike Daley, Matt Dau, Jeffrey Dean, Ben Gelb, Tara Vazir Ghaemmaghami, Rajendra Gottipati, William Gulland, Robert Hagmann, C. Richard Ho, Doug Hogberg, John Hu, Robert Hundt, Dan Hurt, Julian Ibarz, Aaron Jaffey, Alek Jaworski,

- Alexander Kaplan, Harshit Khaitan, Daniel Killebrew, Andy Koch, Naveen Kumar, Steve Lacy, James Laudon, James Law, Diemthu Le, Chris Leary, Zhuyuan Liu, Kyle Lucke, Alan Lundin, Gordon MacKean, Adriana Maggiore, Maire Mahony, Kieran Miller, Rahul Nagarajan, Ravi Narayanaswami, Ray Ni, Kathy Nix, Thomas Norrie, Mark Omernick, Narayana Penukonda, Andy Phelps, Jonathan Ross, Matt Ross, Amir Salek, Emad Samadiani, Chris Severn, Gregory Sizikov, Matthew Snelham, Jed Souter, Dan Steinberg, Andy Swing, Mercedes Tan, Gregory Thorson, Bo Tian, Horia Toma, Erick Tuttle, Vijay Vasudevan, Richard Walter, Walter Wang, Eric Wilcox, and Doe Hyun Yoon. In-dataloader performance analysis of a tensor processing unit. *SIGARCH Comput. Archit. News*, 45(2):1–12, jun 2017.
- [15] Yann LeCun, John S Denker, and Sara A Solla. Optimal brain damage. In *Advances in neural information processing systems*, pages 598–605, 1990.
- [16] Namhoon Lee, Thalaisyasingam Ajanthan, and Philip HS Torr. Snip: Single-shot network pruning based on connection sensitivity. *arXiv preprint arXiv:1810.02340*, 2018.
- [17] Zhuang Liu, Jianguo Li, Zhiqiang Shen, Gao Huang, Shoumeng Yan, and Changshui Zhang. Learning efficient convolutional networks through network slimming. In *Proceedings of the IEEE international conference on computer vision*, pages 2736–2744, 2017.
- [18] Zhuang Liu, Mingjie Sun, Tinghui Zhou, Gao Huang, and Trevor Darrell. Rethinking the value of network pruning. *arXiv preprint arXiv:1810.05270*, 2018.
- [19] Jian-Hao Luo, Jianxin Wu, and Weiyao Lin. Thinet: A filter level pruning method for deep neural network compression. In *Proceedings of the IEEE international conference on computer vision*, pages 5058–5066, 2017.
- [20] Esteban Real, Alok Aggarwal, Yanping Huang, and Quoc V Le. Regularized evolution for image classifier architecture search. In *Proceedings of the aaai conference on artificial intelligence*, pages 4780–4789, 2019.
- [21] Alex Renda, Jonathan Frankle, and Michael Carbin. Comparing rewinding and fine-tuning in neural network pruning. *arXiv preprint arXiv:2003.02389*, 2020.
- [22] Mark Sandler, Andrew Howard, Menglong Zhu, Andrey Zhmoginov, and Liang-Chieh Chen. Mobilenetv2: Inverted residuals and linear bottlenecks. In *Proceedings of the IEEE conference on computer vision and pattern recognition*, pages 4510–4520, 2018.
- [23] Jingtong Su, Yihang Chen, Tianle Cai, Tianhao Wu, Ruiqi Gao, Liwei Wang, and Jason D Lee. Sanity-checking pruning methods: Random tickets can win the jackpot. *arXiv preprint arXiv:2009.11094*, 2020.
- [24] Mingxing Tan and Quoc Le. Efficientnet: Rethinking model scaling for convolutional neural networks. In *International Conference on Machine Learning*, pages 6105–6114. PMLR, 2019.
- [25] Hidenori Tanaka, Daniel Kunin, Daniel LK Yamins, and Surya Ganguli. Pruning neural networks without any data by iteratively conserving synaptic flow. *arXiv preprint arXiv:2006.05467*, 2020.
- [26] Artem Vysogorets and Julia Kempe. Connectivity matters: Neural network pruning through the lens of effective sparsity. *arXiv preprint arXiv:2107.02306*, 2021.
- [27] Alvin Wan, Xiaoliang Dai, Peizhao Zhang, Zijian He, Yuandong Tian, Saining Xie, Bichen Wu, Matthew Yu, Tao Xu, Kan Chen, et al. Fbnetv2: Differentiable neural architecture search for spatial and channel dimensions. In *Proceedings of the IEEE/CVF Conference on Computer Vision and Pattern Recognition*, pages 12965–12974, 2020.
- [28] Chaoqi Wang, Guodong Zhang, and Roger Grosse. Picking winning tickets before training by preserving gradient flow. *arXiv preprint arXiv:2002.07376*, 2020.
- [29] Hongxu Yin, Pavlo Molchanov, Jose M Alvarez, Zhizhong Li, Arun Mallya, Derek Hoiem, Niraj K Jha, and Jan Kautz. Dreaming to distill: Data-free knowledge transfer via deepinversion. In *Proceedings of the IEEE/CVF Conference on Computer Vision and Pattern Recognition*, pages 8715–8724, 2020.
- [30] Dongzhan Zhou, Xinchu Zhou, Wenwei Zhang, Chen Change Loy, Shuai Yi, Xuesen Zhang, and Wanli Ouyang. Eonas: Finding proxies for economical neural architecture search. In *Proceedings of the IEEE/CVF Conference on computer vision and pattern recognition*, pages 11396–11404, 2020.
- [31] Shuchang Zhou, Yuxin Wu, Zekun Ni, Xinyu Zhou, He Wen, and Yuheng Zou. Dorefa-net: Training low bitwidth convolutional neural networks with low bitwidth gradients. *arXiv preprint arXiv:1606.06160*, 2016.
- [32] Barret Zoph and Quoc V Le. Neural architecture search with reinforcement learning. *arXiv preprint arXiv:1611.01578*, 2016.

A Proof of SynExp Invariance Theorem

Theorem 1. *Given a specific CNN architecture, the SynExp ($\mathbb{E}_{[M,W]}[\mathcal{S}_{\text{SF}}]$) of any randomly compressed model with the same layer-wise density p_l is a constant, independent of the pruning granularity. The constant SynExp equals to:*

$$\mathbb{E}_{M,W}[\mathcal{S}_{\text{SF}}] = NC_{N+1} \prod_{l=1}^N (p_l C_l \cdot \mathbb{E}_{x \sim \mathcal{D}}[|x|]), \quad (7)$$

where N is the number of layers in the network, $\mathbb{E}_{x \sim \mathcal{D}}[|x|]$ is the expectation of magnitude of distribution \mathcal{D} , C_l is the input channel size of layer l and is also the output channel size of $l-1$, and $p_l = \frac{1}{\alpha_l} \|M_l\|_0$ is the layer-wise density.

Proof. Assuming the network has N layers, weight matrix $W^l \in \mathbb{R}^{m_l \times n_l}$, mask matrix $M^l \in \{0, 1\}^{C_l \times C_{l+1}}$. C_l and C_{l+1} are the input and output channel size of layer l . As the output channel size of any layer l equals to the input channel size of the next layer $l+1$, we have $C_{l+1} = C_l, \forall l < N$.

We first prove the Theorem 1 on fully-connected network, and we can extend it to CNNs easily. From Equation 1, in a fully-connected network, the Synaptic Flow score for any parameter W_{ij}^l with mask M_{ij}^l in layer l equals to:

$$\mathcal{S}_{\text{SF}}(W_{(i,j)}^l) = \left[\mathbf{1}^T \prod_{k=l+1}^N |W^k \odot M^k| \right]_i |W_{(i,j)}^l M_{(i,j)}^l| \left[\prod_{k=1}^{l-1} |W^k \odot M^k| \mathbf{1} \right]_j \quad (8)$$

We compute the SynExp of the layer l ($\mathbb{E}_{[M,W]}(\mathcal{S}_{\text{SF}})^{[l]}$), then the SynExp of the network is simply the sum of SynExp of all layers:

$$\mathbb{E}_{[M,W]}(\mathcal{S}_{\text{SF}}) = \sum_{l=1}^N \mathbb{E}_{[M,W]}(\mathcal{S}_{\text{SF}})^{[l]} \quad (9)$$

We define the expectation value for input channel i , output channel j , and the whole layer in layer l as $E_{(i,*)}^l$, $E_{(*,j)}^l$, and $E_{(*,*)}^l$:

$$\mathbb{E}_{(i,*)}^l = \frac{1}{C_{l+1}} \sum_x |W_{(i,x)}^l M_{(i,x)}^l| \quad (10)$$

$$\mathbb{E}_{(*,j)}^l = \frac{1}{C_l} \sum_x |W_{(x,j)}^l M_{(x,j)}^l| \quad (11)$$

$$\mathbb{E}_{(i,j)}^l = \mathbb{E}_{(*,*)}^l = \frac{1}{C_l C_{l+1}} \sum_{i,j} |W_{(i,j)}^l M_{(i,j)}^l| = \frac{1}{\alpha_l} \sum_{i,j} |W_{(i,j)}^l M_{(i,j)}^l| = p_l \mathbb{E}_{|\mathcal{D}^l|} \quad (12)$$

Here we use $\mathbb{E}_{|\mathcal{D}^l|}$ to denote $\mathbb{E}_{x \sim \mathcal{D}}[|x|]$.

As the weight in layer l is sampled from distribution \mathcal{D} , and the mask matrices are also randomly sampled, we have

$$\mathbb{E}_{(*,*)}^{[k]} = \mathbb{E}_{(i,*)}^k = \mathbb{E}_{(*,j)}^k = p_l \mathbb{E}_{|\mathcal{D}^l|} \quad (13)$$

With $E_{(i,*)}^k$, $E_{(*,j)}^k$, and $E_{(*,*)}^k$, we can rewrite Equation 8 to:

$$\mathbb{E}[\mathcal{S}_{\text{SF}}(W_{(i,j)}^l)] = \left(\prod_{k=l+2}^N C_{k+1} \mathbb{E}_{(*,*)}^k \right) \cdot C_{l+2} \mathbb{E}_{(i,*)}^{l+1} \cdot \mathbb{E}_{(i,j)}^l \cdot C_{l-1} \mathbb{E}_{(*,*)}^{l-1} \cdot \left(\prod_{k=1}^{l-2} C_k \mathbb{E}_{(*,*)}^k \right) \quad (14)$$

Combining Equation 3 and 14, because the instantiation of the weight matrices and mask matrices for each layer are independent:

$$\begin{aligned}
\mathbb{E}_{[M,W]}(\mathcal{S}_{\text{SF}})^{[l]} &= \mathbb{E} \left[\sum_{i=1}^{C_l} \sum_{j=1}^{C_{l+1}} \mathcal{S}_{\text{SF}}(W_{(i,j)}^l) \right] = \sum_{i=1}^{C_l} \sum_{j=1}^{C_{l+1}} \mathbb{E} \left[\mathcal{S}_{\text{SF}}(W_{(i,j)}^l) \right] \\
&= \left(\prod_{k=l+2}^N p_k C_{k+1} \mathbb{E}_{|\mathcal{D}^k|} \right) \sum_{i=1}^{C_l} \sum_{j=1}^{C_{l+1}} \left(p_{l+1} C_{l+2} \mathbb{E}_{(i,*)}^{l+1} \cdot p_l \mathbb{E}_{|\mathcal{D}^l|} \cdot p_{l-1} C_{l-1} \mathbb{E}_{(*,j)}^{l-1} \right) \left(\prod_{k=1}^{l-2} C_k \mathbb{E}_{|\mathcal{D}^k|} \right) \\
&= \left(\prod_{k=l+2}^N p_k C_{k+1} \mathbb{E}_{|\mathcal{D}^k|} \right) C_l C_{l+1} \left(p_{l+1} C_{l+2} \mathbb{E}_{|\mathcal{D}^{l+1}|} \cdot p_l \mathbb{E}_{|\mathcal{D}^l|} \cdot p_{l-1} C_{l-1} \mathbb{E}_{|\mathcal{D}^{l-1}|} \right) \left(\prod_{k=1}^{l-2} p_k C_k \mathbb{E}_{|\mathcal{D}^k|} \right) \\
&= C_{N+1} \prod_{l=1}^N (p_l C_l \mathbb{E}_{|\mathcal{D}^l|})
\end{aligned} \tag{15}$$

According to Equation 9,

$$\begin{aligned}
\mathbb{E}_{[M,W]}(\mathcal{S}_{\text{SF}}) &= \sum_{l=1}^N C_{N+1} \prod_{l=1}^N (C_l \mathbb{E}_{|\mathcal{D}^l|}) \\
&= N C_{N+1} \prod_{l=1}^N (p_l C_l \cdot \mathbb{E}_{x \sim \mathcal{D}}[|x|]),
\end{aligned} \tag{16}$$

SynExp Invariance Theorem can also be extended to CNNs, as it is obvious that SynExp of CNNs is proportional to that of fully connected networks. Thus the difference of SynExp between CNNs and fully connected networks for each layer is only a factor equal to $\frac{K^2}{C_{l+1}}$, where K is the kernel size of the convolutional layer. \square

B Solution of the Optimization problem

For the convex optimization problem in Equation 5, Equation 6, or PreConfig, we can simply use Karush–Kuhn–Tucker (KKT) conditions to analytically solve it. We include the solutions as follows for completeness.

B.1 Optimization with Parameter Count Constraint

$$\begin{aligned}
p_l &= \min\left(\frac{\mu}{\alpha}, 1\right) \\
\text{where } \mu \text{ satisfies: } &\sum_{l=1}^N \min(\alpha_l, \mu) = B_{\text{params}}
\end{aligned} \tag{17}$$

B.2 Optimization with Parameter Count and FLOPs Constraints

$$\begin{aligned}
p_l &= \min\left(\frac{1}{\mu_1 \alpha_l + \mu_2 \beta_l}, 1\right) \\
\text{where } \mu_1, \mu_2 \text{ satisfy: } &\sum_{l=1}^N \alpha_l \min\left(\frac{1}{\mu_1 \alpha_l + \mu_2 \beta_l}, 1\right) = B_{\text{params}} \\
&\sum_{l=1}^N \beta_l \min\left(\frac{1}{\mu_1 \alpha_l + \mu_2 \beta_l}, 1\right) = B_{\text{flops}}
\end{aligned} \tag{18}$$

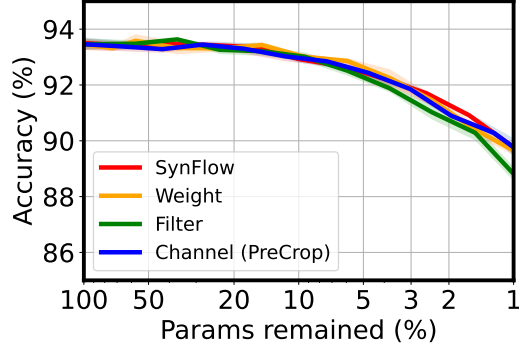


Figure 6: Comparison of the performance using different pruning granularities on VGG16 using CIFAR-10.

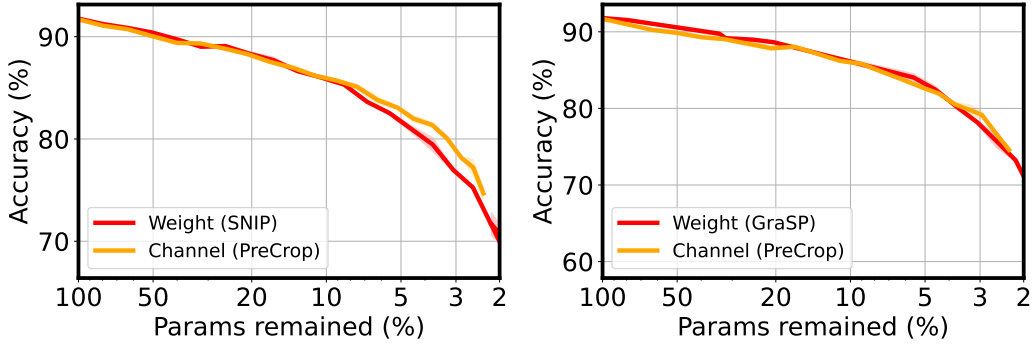


Figure 7: Comparison of the performance using different pruning granularities on ResNet20 using CIFAR-10. SNIP (left) and GraSP (right) importance scores are used.

B.3 Formulation of PreConfig

$$\begin{aligned}
 p_l &= \frac{1}{\mu_1 \alpha_l + \mu_2 \beta_l} \\
 \text{where } \mu_1, \mu_2 \text{ satisfy: } &\sum_{l=1}^N \alpha_l \frac{1}{\mu_1 \alpha_l + \mu_2 \beta_l} = B_{\text{params}} \\
 &\sum_{l=1}^N \beta_l \frac{1}{\mu_1 \alpha_l + \mu_2 \beta_l} = B_{\text{flops}}
 \end{aligned} \tag{19}$$

In practice, to avoid solving the μ , we use a convex optimization solver, which can obtain the solution with a CPU within a second for such a small scale convex optimization.

C More Empirical Results on SynExp Invariance Theorem

We show more empirical results that validates SynExp Invariance Theorem. We first show the comparison of the performance using different pruning granularities on VGG16 using CIFAR-10. All the settings in this experiment is the same as in Figure 1, except this experiment is done on VGG16.

Then we also verify that SynExp Invariance Theorem not only holds for SynFlow, but also holds for other PAI algorithms. In this experiment, we first use other PAI (i.e., SNIP and GraSP) to obtain the layerwise density p_l . Then we use random pruning to match p_l in the channel level. The results are shown in Figure 7.

As shown in all the above experiments, as long as the layerwise density is the same, the pruning granularities do not affect the model accuracy.

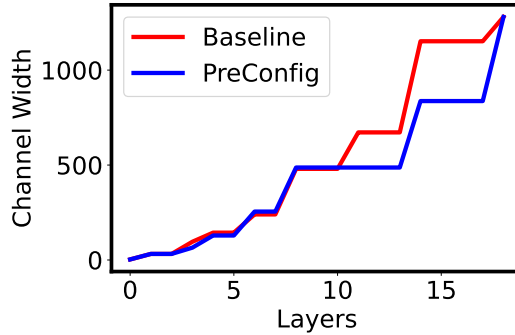


Figure 8: Comparison of the channel width of EfficientNetB0 before and after PreConfig.

D Channel Width Comparison

We also include a comparison of the channel width between the baseline EfficientNetB0 and PreConfig EfficientNetB0 in Figure 8.

E Experiment Details

E.1 Implementation

We adapt model implementations of ResNet, ShuffleNet, and MobileNetv2 from [imgclsmob](https://github.com/osmr/imgclsmob)². The implementations of SynFlow, SNIP, and GraSP are based on the codebase of SynFlow³.

E.2 Hyperparameters

Here we provide the hyperparameters used in training all models in Table 3. No AutoAugment, Label Smoothing, or stochastic depth is used during training. All the CIFAR-10 models are trained with same hyperparameter setting.

Table 3: Hyperparameters used in training.

	CIFAR-10	ImageNet		
		MobileNet	ResNet	EfficientNet
Optimizer	momentum	momentum	momentum	momentum
Training Epochs	160	180	90	150
Batch Size	128	256	512	256
Initial Learning Rate	0.1	0.025	0.2	0.035
Learning Rate Schedule	linear	drop at each epoch	drop at 30, 60 epoch	drop at each epoch
Drop Rate	N.A.	0.98	0.1	0.99
Weight Decay	10^{-4}	4×10^{-5}	10^{-4}	4×10^{-5}

²<https://github.com/osmr/imgclsmob>

³<https://github.com/ganguli-lab/Synaptic-Flow>